Int. J. Electrochem. Sci., 17 **(2022)** Article Number: 22046, doi: 10.20964/2022.04.50

International Journal of
ELECTROCHEMICAL
SCIENCE
www.electrochemsci.org

Preparation and Research of new Polyelectrolyte based on $Li_{1.3}Al_{0.3}Ti_{1.7}(PO_4)_3$ for all solid state batteries

Xinghua Liang, Xingtao Jiang, Dayong Yang[*]*, Yu Zhang , Lingxiao Lan*[*] *Zhenjiang Wang*

Guangxi Key Laboratory of Automobile Components and Vehicle Technology, Guangxi University of Science & technology, Liuzhou 545006, China;
[*]E-mail: dyyang@gxust.edu.cn (Dayong Yang), 350926068@qq.com (Lingxiao Lan)

Received: 4 November 2021 / *Accepted:* 27 January 2022 / *Published:* 4 March 2022

Solid-state lithium batteries have attracted more and more attention due to their higher safety and energy density. Solid electrolytes are the key materials of solid-state lithium batteries. Therefore, the development of solid-state electrolytes with high ionic conductivity is the key to the development of solid-state batteries. In this work, a simple method was successfully used to prepare a Polysulfone（PES）-based composite solid electrolytes (CSEs) is developed. The prepared CSE PES @Li-10% $Li_{1.3}Al_{0.3}Ti_{1.7}(PO_4)_3$（LATP）has an ionic conductivity of 5.37×10^{-4} Scm^{-1} and a wide electrochemical window of 5.213 V in a greenhouse. A pair of lithium-ion batteries were assembled to maintain good cycling stability at three current densities of 0.05 $mAcm^{-2}$, 0.1 $mAcm^{-2}$ and 0.2 $mAcm^{-2}$. After the Li/PES@Li-10%LATP/$LiNi_{0.5}Mn_{1.5}O_4$ cells were assembled and tested at room temperature, the discharge capacity of the cathode in the first circle was 121.8 mAh/g. After 50 cycles at room temperature, the discharge capacity of the cathode remained at 119.51 mAh/g, with a coulombic efficiency of 97 %. At 0.1 C and 0.2 C, 0.3 C and 0.5 C and 1C ratio in circulation, the cathode discharge capacity of 121.8 mAh/g, respectively 93.5mAh/g, 72.1 mAh/g, 36.5 mAh/g and 21.6 mAh/g, and multiplying power cycle stability. The research provides a basis for the development of all-solid-state batteries at room temperature.

Keywords: $Li_{1.3}Al_{0.3}Ti_{1.7}(PO_4)_3$, $LiNi_{0.5}Mn_{1.5}O_4$, room temperature, first circle, all-solid-state batteries.

1. INTRODUCTION

Rechargeable lithium (Li)-metal battery with considerable energy density is one of the most promising candidates for next generation energy storage system [1–3]. Although it is widely used in various devices, it still plagues traditional lithium batteries due to safety issues such as leakage and flammability [4-6].In order to overcome various defects, solid-state batteries with solid electrolytes with higher safety and flexibility have been designed in recent years [7-10].In addition, the wide chemical

window can not only match the excellent cathode materials, but also improve the total energy density of the battery [11-15].

All solid-state batteries are generally divided into three types: inorganic solid electrolyte, organic polymer solid electrolyte and inorganic-organic composite solid electrolyte [16-19].Inorganic solid electrolytes mainly include $Li_7La_3Zr_2O_{12}$（LLZO）, LATP, LAGP and various derivatives.The ionic conductivity of superionic conductors such as LATP, solid electrolyte with NASICON structure, is high and can reach more than 10^{-4} S/cm [20-23].The ionic conductivity of sulfide electrolytes (such as $Li_{10}GeP_2S_{12}$) can even reach 10^{-2} S/cm [24,25], which can be comparable to the conductivity of liquid electrolytes, but sulfides are unstable in the air, and will produce toxic gas H_2S after absorbing water [26].Although the garnet type electrolyte LLZO is stable to lithium metal [27], it is also unstable to air [28-30], resulting in other products that affect its ionic conductivity and interface impedance with the electrode.The bulk ionic conductivity and total ionic conductivity of the NASICON electrolyte LATP can reach 10^{-3} S/cm, 7×10^{-4} S/cm [31-33], which can meet the requirements of all-solid-state battery for ionic conductivity. Moreover, it is stable to air and water [34,35], and can be used for large-scale preparation of materials in air atmosphere, and battery assembly, which reduces processing difficulty and production costs.However, large interface impedance and side reactions make them difficult to directly apply. In CSEs, PVDF, PEO, PVC and so on are widely used. However, generally, the ionic conductivity of CSEs at room temperature ($< 10^{-5}$ S/cm) and cation migration number are low, and some CSEs have poor oxidation resistance [36-38]. A single polymer is usually at room temperature.It exhibits low conductivity and poor electrochemical performance, so it is difficult to match with other substances.So far, people have focused on adding buffer layer on the surface of solid electrolyte, polymerization of various polymers and design of multilayer CSE. Although these methods can effectively improve the cycling performance of solid electrolyte, the preparation process is complex and the cost is high, which is still a certain gap compared with large-scale use.

In contrast, the combination of inorganic and organic in a solid electrolyte not only improves the conductivity, but also greatly improves the mechanical properties. We use the new polymer PES as the substrate, which has excellent mechanical properties and thermoplastic. And has excellent electrical properties, insulation stability at 200 ℃.

In this work, PES polymer was used as the substrate to form a blend CSE with disordered lithium salt $LiBF_4$ and inorganic solid electrolyte LATP. The optimum ratio of LATP was determined and the CSE PES@Li-10 % LATP was found to have good properties. Electrochemical tests showed that there was no short circuit after 300 cycles of lithium stripping experiment at room temperature, and it showed good cycling stability. By assembling into $LiNi_{0.5}Mn_{1.5}O_4$/PES@Li-10%LATP/Li, after 50 cycles, it still maintains a coulombic efficiency of 97 %.The prepared CSE PES@Li-10%LATP provides a strong basis for the development of all solid-state points at room temperature.

2. EXPERIMENTAL SECTION

2.1. Preparation of LATP powder

In the solid-phase method, lithium carbonate (Li_2CO_3), aluminum oxide (Al_2O_3), titanium dioxide (TiO_2) and ammonium dihydrogen phosphate ($NH_3H_2PO_4$) zinc oxide (ZnO) were used as

predispositions and weighed according to the stoichiometric ratio of $Li_{1.3}Al_{0.3}Ti_{1.7}(PO_4)_3$. The mixture was evenly mixed and the ball mill was milled for 8h with ethanol as dispersant and the speed of the mill was 280 r/min.After ball milling, the powder was dried in a drying oven at 80℃ for 10h. After ethanol volatilization, the powder was ground for 1h and sieved with 160 mesh fine powder sieve. The powder was annealed and calcined at 950 ℃ for 4h in an atmosphere furnace to obtain white LATP precursor powder.

2.2. Preparation of PES@Li-10％LATPcomposite electrolytes

Preparation of solid electrolyte membrane PES@Li-10%LATP. First, add 20 mL N,N-Dimethylformamide（DMF） solution to a 100 mL beaker and stir with electric at 60 ℃. Add 4g PES until the solution becomes a sol solution, continue to add $LiBF_4$ (PES: $LiBF_4$ = 8:1) until the mixture is stirred without bubbles, then add 0.4 g LATP and stir for 12 h.Then pour it into a teflon container and dry it at 60 ℃ for 12h in a blowing drying oven. Then cut it to 16mm and put it in a glove box for later use. Marked as PES@Li-10 ％LATP. At the same time, the content of solid electrolyte LATP was changed, adding 5 % and 15 %LATP. Marked as PES@Li-5％LATP and PES@Li-15%LATP. Compare as a control. In Table 1, the abbreviations PVDF, PMMA, PEO used are poly(1,1-difluoroethylene), poly(1,1-difluoroethylene) and Poly(ethylene oxide), respectively, compared with the polymers in the reference.

2.3. Preparation of solid-state $LiNi_{0.5}Mn_{1.5}O_4$/PES@Li-10％LATP/Li cell

The CR 2032 button battery is assembled in an argon filled glove box using the above composite SSE. Cathode active material were prepared by mixing 80 wt% commercial $LiNi_{0.5}Mn_{1.5}O_4$ (Aales Shanghai Co, LTD.), 10 wt% conductive carbon black and 10 wt% PVDF dissolved in NMP solvent. After complete mixing, the cathode active material slurry is evenly cast onto the aluminum foil. Then the aluminum foil was dried under a vacuum at 110 ℃ and then cut into a circular electrode with a diameter of 12mm. The battery is assembled by a positive shell, a positive plate, an electrolyte, a lithium, a steel plate, a shrapnel and a negative shell. In addition, a small amount of electrolyte is added on both sides of the CSE to improve the interface. The electrochemical performance of all assembled cells in the 2032 battery test system is characterized by a voltage range of 3.5-5 V.

2.4. Physical characterizations

By using the phase structure of X-ray diffraction (XRD), test data were collected at 10-90°. The surface and structure of inorganic solid electrolyte LATP were observed by field emission scanning electron microscopy (SEM, JSM-7001F,Japan).

2.5. Electrochemical measurements

Lithium ion transfer number (t_{Li^+}) is an important parameter for evaluating the performance of composite electrolytes. A higher t_{Li^+} value indicates that more lithium ions are involved in the electrochemical cycle. Typically, the test is performed by timing on a lithium symmetric cell (e.g. Li/PPLL/Li) at a voltage of 1mV for 4000 s, and the t_{Li^+} value is calculated by the following equation.Combined with the measurement method of CV and constant voltage DC polarization, calculated by the publicity.

$$t_{Li^+} = \frac{I_s(\Delta V - I_0 R_0)}{I_0(\Delta V - I_s R_s)}$$

The lithium ion migration number of electrolyte at the test temperature can be obtained. t_{Li^+} represents the number of lithium ion migration of the electrolyte,I_0 and $I_s$are current values after dc polarization initiation and stabilization respectively, R_0 and $R_s$are impedance values before and after DC polarization respectively, ΔV is the voltage value acting on both ends of the battery.

Ionic conductivity test, cell assembly with steel sheet (SS) as a symmetrical cell, together with electrochemical impedance test, calculate ionic conductivity.

$$\sigma = {}^{L}/_{(R \times S)}$$

The ionic conductivity of the electrolyte at the test temperature can be obtained. Among them, σ represents the ionic conductivity, L is the thickness of the electrolyte, S represents the contact area between the electrolyte and the test electrode (SS), and R denotes the bulk impedance value of the battery electrolyte measured by EIS.

The electrochemical window test was carried out by linear sweep voltammetry (LSV) to obtain the electrochemical stability window of electrolyte membrane. Lithium sheet was used as counter electrode and reference electrode, stainless steel sheet was used as working electrode (SS), and electrolyte membrane was in the middle (Li/PIL/SS). The test range was 0 V-6 V, and the sweep speed was 0.5 mVs^{-1}.

Li/PES@Li-10%LATP/Li battery was assembled to conduct lithium stripping experiment. At the same time, $LiNi_{0.5}Mn_{1.5}O_4$/PES@Li-10%LATP/Li battery was assembled to test CV and cycle rate.

3. RESULTS AND DISCUSSION

Firstly, the prepared LATP particles were characterized. Figure 1a shows that the crystal structure of the prepared LATP is obvious and the particle size ranges from 1 μm to 5 μm.This is consistent with the LATP morphology previously reported. The particle distribution of the sample is relatively uniform, the morphology is complete, the degree of agglomeration is low, and the boundary is clear. The ball milling process makes the sample structure more compact, good dispersion, smooth sample surface, and high density. Figure 1b shows the prepared polymer the topography of the CSE, which is laid flat on the PTFE board, shows that the CSE has high film-forming properties, and the prepared CSE is tested. We test XRD between different polymers. In Figure 1c, we see the XRD of the two polymers, PES and PES@Li. With the addition of lithium salt, we can see that at 24.3°, a LiOH peak is obtained, which indicates that our prepared film When tested in air, Li^+ in the polymer reacts with air to form LiOH,

which shows that the $LiBF_4$ we use can dissolve lithium salts well, and generate free Li^+ and anion groups in the polymer, which can be very good. Transport Li^+. Then we tested the XRD of polymer electrolyte membranes with different contents of LATP (Figure 1d), we can clearly see that when PES@Li was added with LATP, the peak intensity did not increase significantly, indicating that LATP was only mixed into the polymer PES , did not participate in the reaction.

In order to prove the idea that the solid electrolyte LATP can improve the conductivity of the CSE membrane, we further studied the ionic conductivity and electrochemical properties of the PES membrane with different contents. Figure 1e shows the ionic conductivity-temperature curves of CSE membranes with different LATP contents. It can be seen from the curves that the ionic conductivity does increase significantly with the addition of LATP. By comparing the conductivity of LATP electrolyte with different contents, it was found that at the test temperature, the ionic conductivity of the sample with the optimal LATP content of 10wt%.PES@Li-10%LATP reached 5.37×10^{-4} Scm^{-1} at 30 ℃ and 3.76×10^{-3} Scm^{-1} at 70 ℃, while that of the pure PES electrolyte membrane reached 5.37×10^{-4} Scm^{-1} at 70 ℃, PES only reaches $6.87\times10^{-6}Scm^{-1}$ at 30℃. The amorphous region is formed due to acid-base interaction after the addition of lithium salt. When the filler reaches 10% of the mass fraction, the lithium ion just forms a suitable enrichment area, providing continuous channels for the shuttle of lithium ions in CSE.

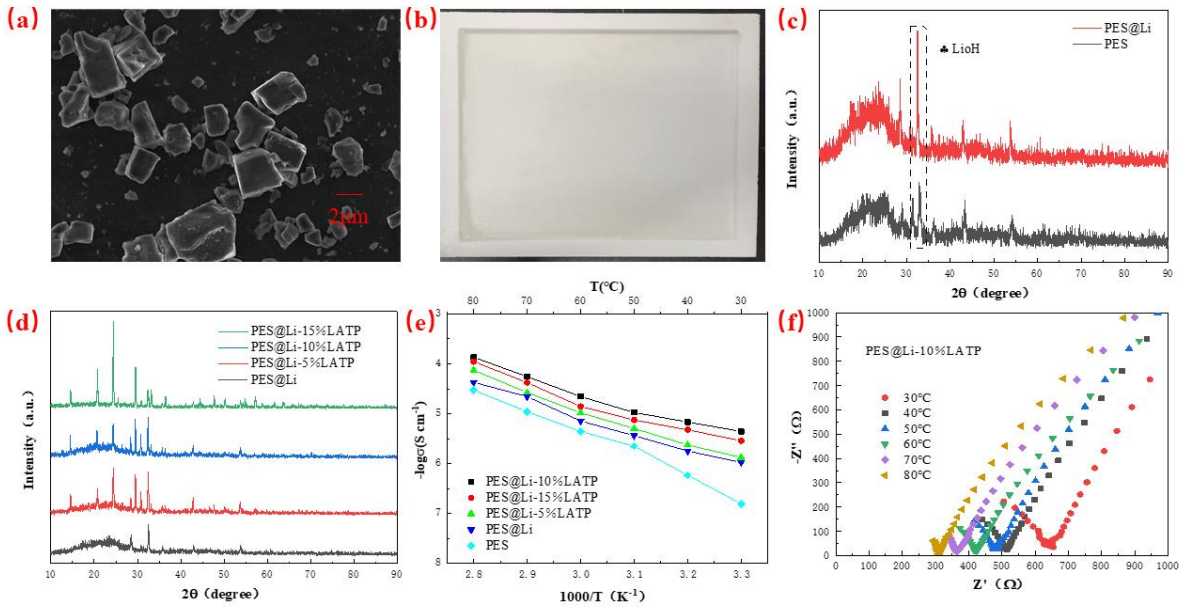

Figure 1.a) SEM image of the fabricated test LATP powder phosphate precursor.b) Topography of CSE. c,d) XRD patterns of different polymer. e) Conductivity of CSE at different temperatures. f) PES@Li-10％LATP impedance diagram at different temperatures.

However, due to the effective mass theory (EMT), the extra inactive filler will hinder the shuttle of lithium ions [39,40]. So our Nyquist curve is shown in the Figure as shown in Figure 1e. Next, in order to visually express the effect of temperature on conductivity, we have made the interface

impedance at different temperatures as shown in Figure 1f. We can observe CSE membrane PES@Li-10%LATP interface impedance under different temperatures, as the temperature continues to increase, the activity of the polymer segment intensifies, and the molecular motion is violent, resulting in a decrease in impedance, so it shows that the conductivity increases with the increase of temperature.

The number of lithium ion migration is an important indicator to measure the performance of CSE.The number of lithium ion migration of PES@Li-10%LATP was calculated by timing current method in Figure 2a combined with CV impedance spectroscopy. Figure 2b at the initial stage of polarization, the motion of Li^+ and BF_4^- contributed current, and only lithium ions shuttled through the CSE after polarization, and the current gradually stabilizes. In the CSE, according to the calculation formula, we get the ion migration number of PES@Li-10%LATP is 0.47. We believe that the high migration number of PES@Li-10%LATP can be attributed to the anion binding effect of LATP on CSE.

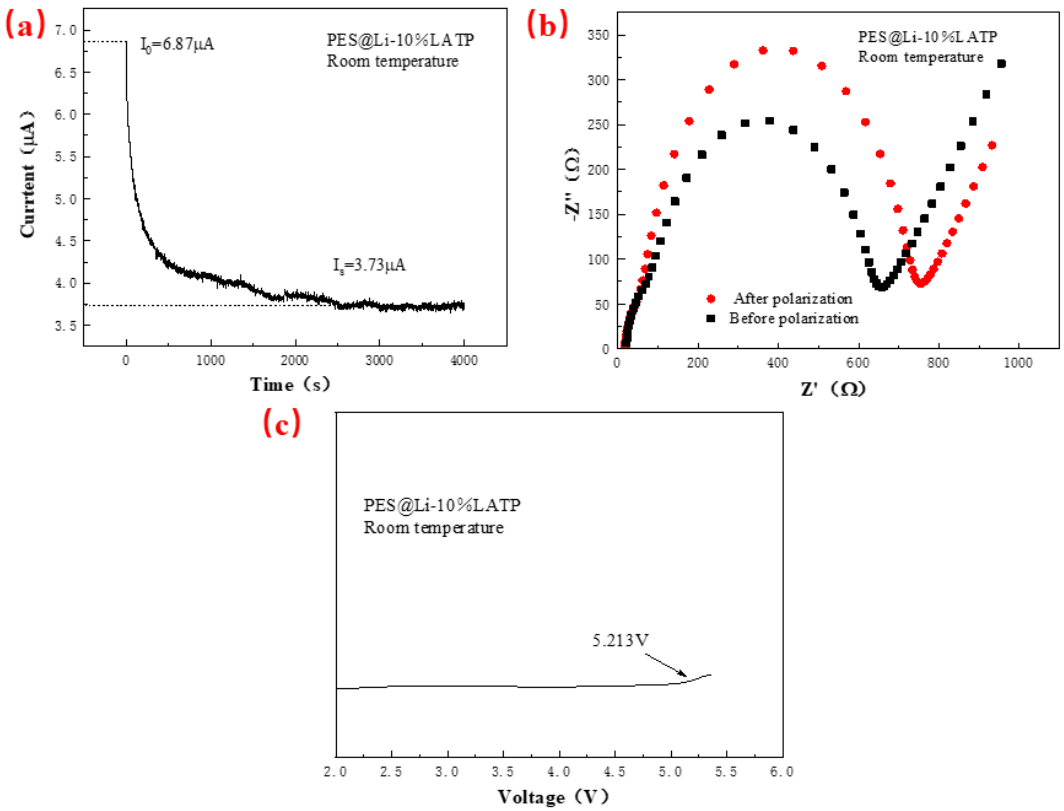

Figure 2.a, b) Chronoamperometry profiles and AC impedance spectra (before and after polarization) of PES@Li-10％LATP. c) PES@Li-10％LATP linear voltammetry test.

In this experiment, we used the cathode material $LiNi_{0.5}Mn_{1.5}O_4$(4.7 V) with a high voltage window. In order to verify whether the prepared PES@Li-10%LATP is suitable for the cathode material, linear sweep voltammetry test (LSV) was carried out, as shown in Figure 2c, and it was concluded that the prepared PES@Li-10%LATP has 5.213 V high voltage window. We believe that in the inorganic solid electrolyte LATP wide electrochemical port and polymer PES can effectively combine to form a

high voltage CSE membrane with organic and inorganic combination. Compared with traditional PEO-based and PVDF-based CSEs, the electrochemical window is significantly improved [41,42].

In order to facilitate the understanding of the performance of CSES prepared by different polymers, we made Table 1 to understand their performance. From the table, we can see that the performance of PEO and PMMA polymer electrolytes is poor at room temperature, and the composite performance of PVDF and PVDF materials is greatly improved at room temperature. These are due to the different performance of different polymers at room temperature. The electrochemical window of the experimentally prepared PES@Li-10%LATP is 5.213 V, which is significantly higher than that of PEO@10 % LATP-$LiPF_6$ and PVDF@LATP-LiTFSI, and the conductivity and t_{Li^+} are also significantly improved. This is attributable to the excellent room temperature performance of PES material, which is compatible with $LiBF_4$ and LATP materials, showing excellent performance [5-10].

Table 1. Performance comparison between different LATP polymers

Composite solid electrolytes	**σ/S • cm^{-1}**	**t_{Li^+}**	**Electrochemical window/V**
PVDF@10PEO-5LATP-5$LiPF_6$(PPLL)	5.42x10^{-4}	0.72	5.27
PEO@10％LATP- $LiPF_6$	7.39x10^{-5}	0.39	5.09
PVDF@LATP- LiTFSI	3.64 x10^{-4}	0.42	4.9
PMMA@LATP-$LiCl_4$	6.94 x10^{-5}	0.37	5.12

The constant current method was used to test the deposition/extraction curve of lithium ions in a symmetrical lithium metal battery (Li/PES@Li-10%LATP/Li), and the stability of the interface between the lithium anode and the solid electrolyte was studied. As shown in Figure 3a, the surface topography of CSE after 300 h cycling is smooth and smooth, indicating that there is a good contact between electrolyte and lithium metal with strong interface stability. Figure 3b the CV impedance spectrum before and after 300 h is also proved that the lithium metal and polymer, have a good contact between impedance to reduce the total impedance and the interface specification, lithium polymer membrane in the reaction and the cathode, completely LATP and PES form between polymer and Li metal completely polymerization with the increase of reaction time. At the same time, a certain stability LATP can have effectively prevent short circuit problems caused by lithium dendrite. The formed polymer system can maintain a high cycle stability and provide support during long-term cycling. Figure 3c and 3d show the curves of 100 and 200 cycles. The curves are stable without curve disorder, indicating that the CSE has good compatibility with Li metal. The 300 h deposition/exhumation curve in Figure 3e shows that CSE has strong cyclic stability and provides effective theoretical support for long cycles.

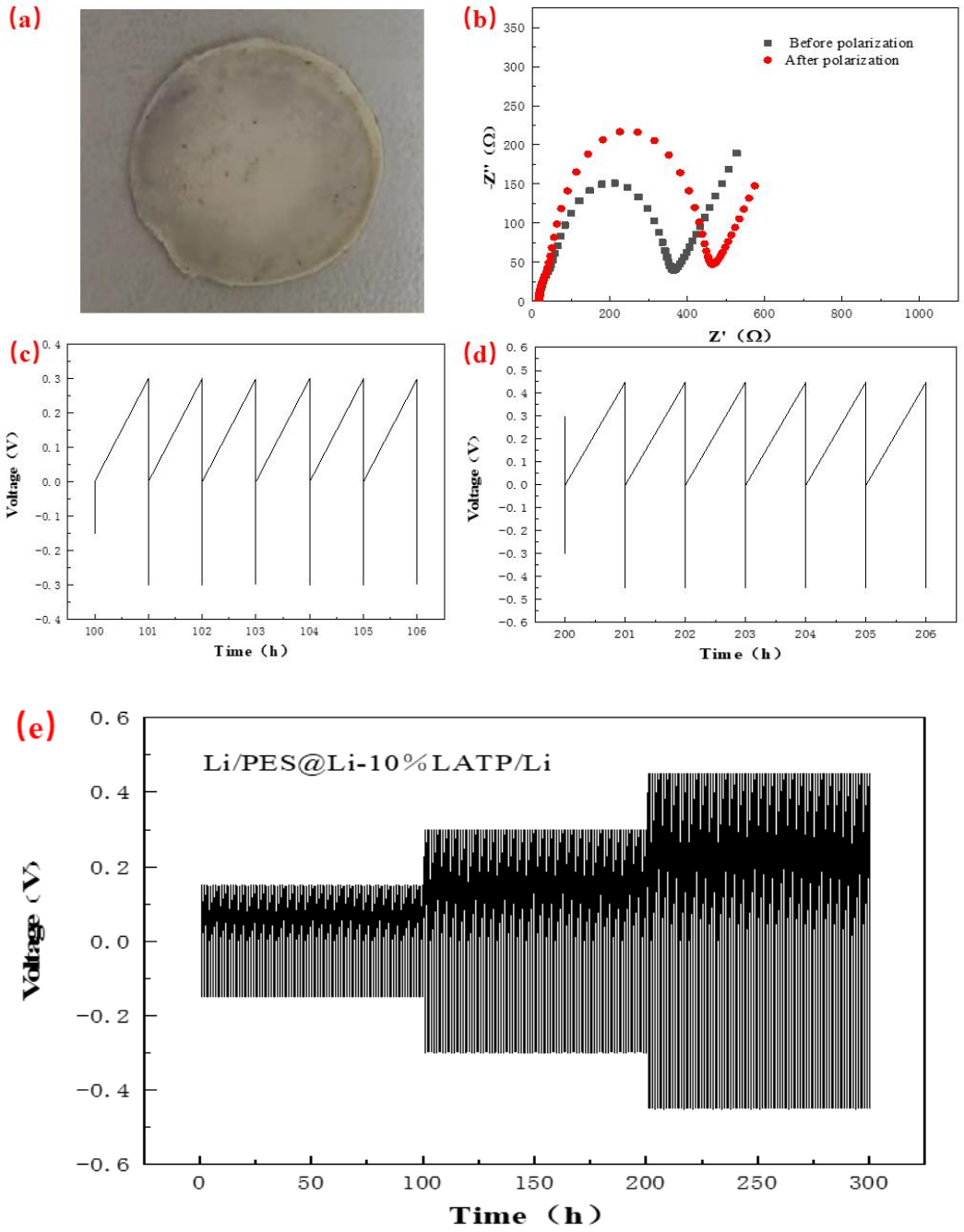

Figure 3. a)PES@Li-10%LATP on the surface after the GCD experiment.b) Impedance diagram of PES@Li-10%LATP after GCD experiment. c, d and e) GCD cycling of the PES@Li-10%LATP at different current density.

In order to test the electrochemical stability of the electrolyte, we assembled a $LiNi_{0.5}Mn_{1.5}O_4$/PES@Li-10%LATP/Li battery and performed a performance test at room temperature. The triple CV cycle at 0.2 mV as shown in Figure 4a shows that the stability of the cycle increases with the increase of the number of cycles. There is little difference in each cycle, indicating that the CSE has a certain cyclic stability in the voltage range of 3.5 V-5 V. Figure 4b shows the first cycle curve at 0.1 C, 0.2 C, 0.3 C and 0.5 C, which is higher than the value reported in previous literature [43]. Figure 4c

shows the five cycle diagrams at different magnifications.It can be seen that the CSE membrane has good cycling stability at different multiplication rates. The discharge specific capacity after 50 cycles has little difference, which is exactly corresponding to Figure 4d. shows that the coulombic efficiency of the battery is 97 % after 50 cycles at 0.1 C at room temperature, which is significantly higher than that of other all-solid-state batteries at room temperature [44].

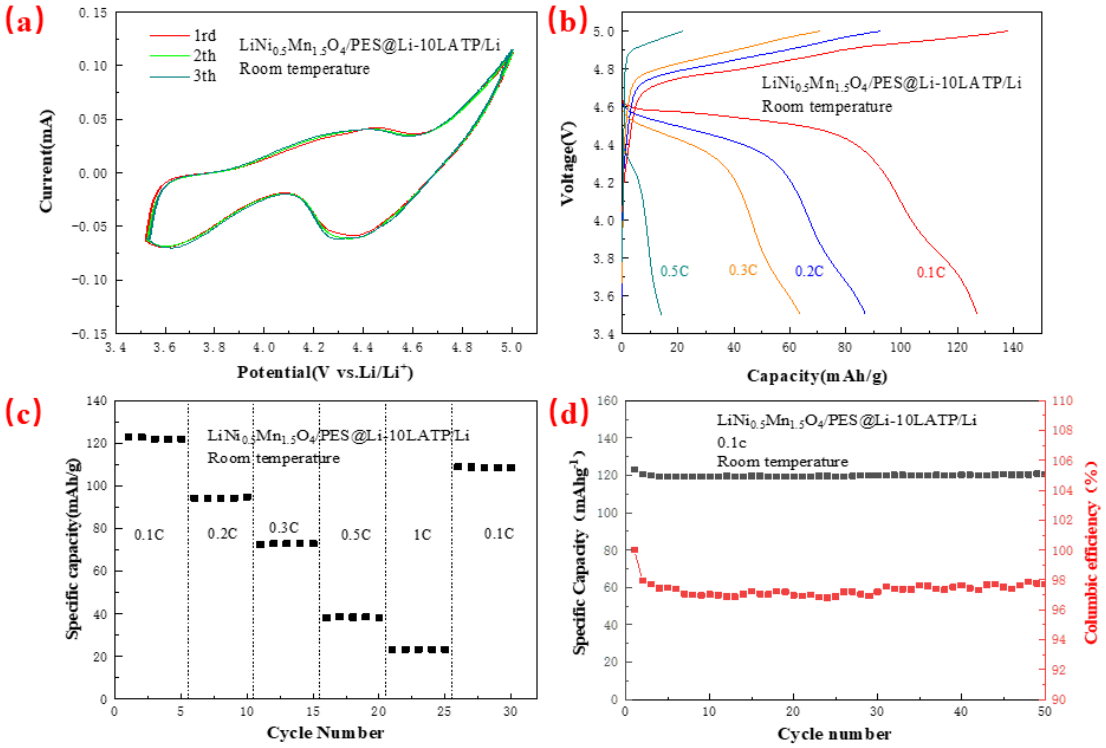

Figure 4. a) CV test of PES@Li-10%LATP battery. b, c) PES@Li-10%LATP battery rate test. d) 100 cycles of PES@Li-10%LATP battery.

4. CONCLUSION

In this work, PES polymer was used as the substrate, and disordered lithium was added to form a copolymer substrate with solid electrolyte LATP. The composite CSE (PES@Li-10%LATP) obtained at room temperature has high ionic conductivity, migration number and wide electrochemical window. The main reason for PES@Li-10%LATP electrolyte is that the PES substrate is very suitable for circulation, and it is relatively stable at room temperature. Amorphous zone is formed after adding disordered lithium salt. At the same time, the addition of LATP has stabilized the stability of CSE. It also provides a channel for continuous transmission of lithium ions. The coulomb efficiency of the prepared $LiNi_{0.5}Mn_{1.5}O_4$/PES@Li-10%LATP/Li cell is 97 % after 50 cycles, and the multiplier performance is good. These results indicate that PES@Li-10%LATP solid electrolyte membranes have a certain potential value in the development of all solid state batteries.

ACKNOWLEDGEMENT
This research was supported by the National Natural Science Foundation of China(No.52161033),Guangxi Natural Science Foundation (No. 2020GXNSFAA297082), the Fund Project of the GDAS Special Project of Science and Technology Development Guangdong Academy of Sciences Program (No.2020GDASYL-20200104030); the Innovation Project of Guangxi University of Science and Technology Graduate Education (YCSW2021324GKYC202112) Guangxi Innovation Driven Development Project (No.AA18242036-2); and the Fund Project of the Key Lab of Guangdong for Modern Surface Engineering Technology(No. 2018KFKT01).Science and Technology Project of Guangxi China (no. GK AD19245149)Science and Technology Project of Liuzhou China (no. 2019DH10601).the National Natural Science Foundation of China (no. 52165055).

Reference

1. X.B. Cheng, C.Z. Zhao, Y.X Yao, H. Liu, Q. Zhang, *Chem.,* 5 (2019) 74.
2. Z.A. Ghazi, Z.H. Sun, C.G. Sun, F. Li, H.M. Cheng, *Small,* 15 (2019) 1900687.
3. L.X. Yuan, L.X. Yuan, K. Yuan, Y. Zhang, Y.Y. Huang, J. Lin, F. Pan, Y.H. Huang, *Joule,* 3 (2019) 2334.
4. S. Yi, T. Xu, L. Li, M. Gao, K. Du, H. Zhao, Y. Zhao, *Solid State Ionics,* 355 (2020) 115419.
5. H.T. Zhang, H. Wu, L. Wang, X.A. Hong, *J. Power Sources,* 492 (2021) 229661.
6. A. Das, M. Goswami, K. Illath, T.G. Ajithkumar, A. Arya, M. Krishnan, *Non-Cryst. Solids,* 558 (2021) 120654.
7. L.S. Li, Y.F. Deng, H.H. Duan, Y.X. Qian, G.H. Chen, *J. Energy Chem.,* 65 (2022) 319.
8. M.C. Long, T. Wang, P.H. Duan, *J. Energy Chem., 65 (2021).*
9. M. Robert, F. Martin, K. Payam, F.R. Dina, G. Olivier, *J. Power Sources,* 489 (2021) 229430.
10. Y. Liang, Y. Liu, D. Chen, L. Dong, *Mater. Today Energy,* 20 (2021) 100694.
11. H. Nagata, Y. Chikusa, *J. Power Sources,* 263 (2014) 141.
12. Y. Hakgyoon, J.S. Han, H.G. Chan, C.J. Sang, J.K. Kim, *Electrochim. Acta,* 365 (2021) 137349.
13. W.J. Qu, M.X. Yan, R. Luo, *J. Power Sources,* 484 (2021) 229195.
14. S. Mahdiyeh, H. Farzaneh, S. Saeed, *J. Colloid Sci.,* 585 (2021) 750.
15. Z.A. Ghazi, Z. Sun, C. Sun, F. Qi, B. An, F. Li, H. Cheng, *Small,* 15 (2019) 1900687.
16. Z. Zhang, Y. Huang, H. Gao, C. Li, J.X. Hang, P.B. Liu, *J. Energy Chem.,* 60 (2021) 259.
17. S. Duluard, A. Paillassa, P. Lenormand, P.L. Taberna, P. Simon, P. Rozier, F. Ansart, J. Ihlefeld, *J. Am. Ceram. Soc.,* 100 (2017) 1.
18. J.N. Liang, S.H. Wang, L. Shuang, L. Jing, *Nano Energy,* 78 (2020) 105107.
19. W.D. Jung, M.J. Jeson, S.S. Shin, J.S. Kim, H.G. Jung, *ACS Omega,* 5 (2020) 26015.
20. H. Wang, P. Hu, X.T. Liu. Y. Shen, L.X. Yuan, Z. Li, Y.H. Huang, *Advanced science,* 20 (2021) 2100684.
21. L.J. Chen, K.M. Song, J. Shi, J.Y. Zhang, L.W. Mi, W.H. Chen, C.T. Liu, C.Y. Shen, *Sci. China Mater.,* 64 (2020) 105.
22. Q.L. Wei, R.H. DeBlock, D.M. Butts, C. Choi, B. Dunn, *Environmental Materials,* 3 (2020) 221.
23. B.Y. Hao, Z. Yang, Y.L. Le, *J. Alloys Compd., 858* (2021) 157716.
24. A.N. Kamay, K.Y. Homma, A.Y. Amakaw, *Nat. Mater.,* 10 (2011) 682.
25. Y. Kato, S. Hori, K. Suzuki, M. Hirayama, A. Mitsui, M. Yonemura, H. Lba, R. Kanno, *Nat. Energy,* 1 (2016) 10630.
26. H. Muramatsu, A. Hayashi, T. Ohtomo, S. Hama, M. Tatsumisago, *Solid State Ionics,* 182 (2011) 116.
27. J.C. Bachman, S Muy, A Grimaud, H.H Chang. *Chemical Reviews,* 116 (2016) 140.
28. G. Larraz, A. Orera, M.L. Sanjuán, *Journal of Materials Chemistry A,* 1 (2013) 11419.
29. W. Xia, B. Xu, H. Duan, Y. Guo, H. Kang, H. Li, H. Liu, *ACS Appl. Mater. Interfaces,* 8 (2016)

5335.
30. W. Xia, B. Xu, H. Duan, Y. Guo, H. Kang, H. Li, H. Liu, *J. Am. Ceram. Soc.,* 100 (2017) 2832.
31. M. Kotobuki, M. Koishi, *J. Am. Ceram. Soc.,* 7 (2019) 69.
32. A. Mertens, S. Yu, N. Schon, *Solid State Ionics,* 309 (2017) 180.
33. H. Aono, E. Sugimoto, Y. Sadaoka, *J. Electrochem, Soc,.* 136 (1989) 590.
34. X.Y. Miao, Q. Xue, S.Y. Huang, *Mater. Lett.,* 289 (2021) 1294171.
35. T. Mitsuharu, K. Riki, Y. Koji, *Mater. Res. Bull.,* 137 (2021) 111178.
36. D. Li, L. Chen, T.S. Wang, L.Z. Fan, *ACS Appl. Mater. Interfaces,* 10 (2018) 7069.
37. L. Yue, J. Ma, J. Zhang, J. Zhao, S. Dong, Z. Liu, G. Cui, L. Chen, *Energy Storage Materials,* 5 (2016) 139.
38. Q. Zhang, K. Liu, F. Ding, X. Liu, *Nano Res.*, 10 (2017) 4139.
39. J. Sax, J.P. Ottino, *Eng. Sci.,* 23 (1983) 165.
40. D.N. Suong T, D.M. Schaetzl, D. Barnali,A.C. Seabaugh, S.K. Fullerton-Shirey, *J. Mater. Chem. C,* 116 (2012) 21216
41. S.X. Deng, B.Q. Wang, Y.F. Yuan, X. Li, Q. Sun, K.D. Davis, M.N. Banis, J.N. Liang, Y. Zhao, J.J. Li, R.Y. Li, T.K. Sham, R.S. Yassar, H. Wang, M. Cai, J. Lu, X.L. Sun, *Nano Energy*, 65 (2019) 103988.
42. M.C. Long, T. Wang, P.H. Duan, *J. Energy Chem., 65 (2021) 236.*
43. S. Deng, B. Wang, Y. Yuan, X. Sun, *Nano Energy,* 65 (2019) 103988.
44. L. Li, Y. Deng, H. Duan, Y. Qian, G. Chen, *J. Energy Chem., 65 (2022) 319.*